EGTRIB Journal
JOURNAL OF
THE EGYPTIAN SOCIETY OF TRIBOLOGY
VOLUME 21, No. 4, October 2024, pp. 59 - 70 **ISSN 2090 - 5882**
(Received July 28. 2024, Accepted in final form August 14. 2024) **jest.journals.ekb.eg**

INFLUENCE OF THE THICKNESS OF THE FRICTION SURFACES ON THE PERFORMANCE OF THE TRIBOELECTRIC NANOGENERATOR

Ali A. S.[1], Al-Kabbany A. M.[2] Ali W. Y.[2] and Ameer A. K.[2]

[1]Mechanical Engineering Dept., Faculty of Engineering, Suez Canal University, EGYPT.
[2]Department of Production Engineering and Mechanical Design, Faculty of Engineering, Minia University, Minia 61111, Egypt.

ABSTRACT
The present study investigates the influence of the thickness of the friction surfaces of the triboelectric nanogenerator (TENG) on the electrostatic charge (ESC). Five types of TENGs were tested where the thickness of the friction materials was variable. Permanent magnets were inserted under one of the contact surfaces.

It was found that ESC drastically decreased with increasing the thickness of contact surface. It may be attributed to the material transfer from one surface to the second one. After contact-separation, it seems that changes in the contact area of the two surfaces can change the magnitude of charging. At sliding, severe rubbing of materials introduces strains that disturb the electrons and reverse their transfer direction. As the thickness of the rubbed surfaces increases, the deformation increases. In addition to that, internal strains in the matrix of the material may alter the charge transfer direction. In presence of magnetic field, voltage increased with increasing the field intensity.

KEYWORDS
Triboelectric nanogenerator, thickness of friction surface, permanent magnet.

INTRODUCTION
The influence of the magnetic field lines and their direction on ESC of the proposed TENG were studied, [1 - 8]. It was revealed that the highest ESC was observed when the moving electrode cut perpendicularly the highest number of the magnetic field lines. Besides, it was found that the direction of sliding displayed significant effect on the generated ESC. It was known that the performance of the TENG based on triboelectrification and magnetic field depends on the position of the permanent magnets relative to the contact area. It was observed that ESC is generated when the lines of a magnetic field are cut by the electrode. It was recommended to select the optimal position of the magnet to harvest the highest voltage. In addition to that, steel sheets were inserted between the permanent magnets and the contact area to distribute the lines of magnetic field, where the steel sheets of different thickness can redirect the magnetic field lines of the magnet and provided extra magnetic field.

The disadvantages of triboelectrification are fires and destruction of electronics, [9 - 13]. It was observed that, blending of two materials of different charges can reduce ESC, [14 - 16]. In medical field, it can be used to repel viruses, [17 - 21], and enhance the performance of TENG, [22 - 24]. Triboelectrification strengthened by electrostatic induction could develop the performance of TENG in energy harvesters, [25 - 28], self-powered sensors, [29 - 31], as well as hybrid electromagnetic-TENG, [32 - 36].

The present work investigates the effect of the thickness of the friction surfaces of the TENG on the ESC. Besides, permanent magnets were inserted under the friction surface.

EXPERIMENTAL

The tested TENG in the present work consisted of the first surface made of silicon rubber of different thickness ranging between 0.1 and 5.0 mm adhered to Al sheet of 0.05 mm thickness representing the first electrode. The second surface was polyamide (PA) of 0.08 mm thickness adhered to Al sheet (second electrode) installed in one surface of wooden cube, Fig. 1. Permanent magnets of 120 and 240 mG field intensity were inserted under the Al sheet, Fig. 2. In the second and third TENG PA was replaced by Al film of 0.05 mm thickness as well as PMMA sheet of 2.0 mm thickness respectively. The dimensions of PMMA were 40 mm long and 22.5 mm width. The fourth TENG contained Al film of different thickness sliding on PMMA sheet of 2.0 mm thickness adhered to 2.0 mm thickness of sponge polyurethane, (PU), where the magnet was inserted, Fig. 3. The fifth TENG included PA of different thickness (the first dielectric) adhered to Al film (the first electrode) sliding on polytetrafluoroethylene (PTFE) film (the second dielectric) of 0.025 mm thickness adhered to the PU sheet, Fig. 4. PA was adhered to wooden cube of 45 × 45 × 45 mm^3 through Al film. A digital voltmeter was used to measure electrostatic charge ((ESC) in volts after contact-separation as well as sliding on the two sliding surfaces. The load value was 10.5 N. In contact-separation, the two surfaces were loaded to each other for five second and separated, then ESC was measured. While at sliding, the distance was 100 mm.

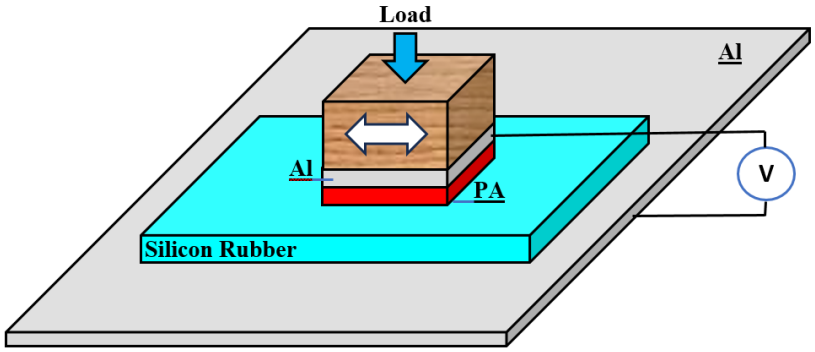

Fig. 1 Arrangement of the test procedure.

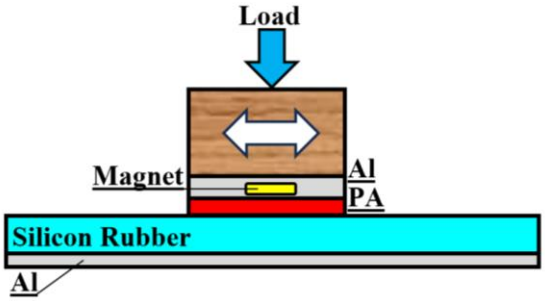

Fig. 2 Arrangement of the tested TENG provided by permanent magnet.

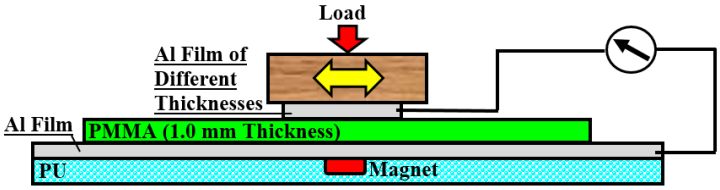

Fig. 3 Arrangement of the fourth tested TENG.

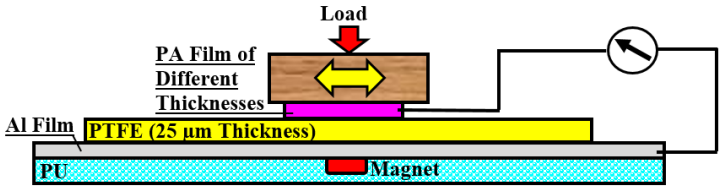

Fig. 4 Fig. 3 Arrangement of the fifth tested TENG.

RESULTS AND DISCUSSION

The relationship between ESC measured by voltage after contact-separation of PA and SR under the effect of the permanent magnets is shown in Fig. 5. Voltage significantly increased up to maximum at 0.2 mm then drastically decreased with increasing SR thickness. Besides, voltage increased with increasing the magnetic field. The values of voltage were 3670, 3400 and 3040 mV at 0, 120 and 240 mG magnetic field respectively. Based on that observation, it can be indicated that the increase of the generated voltage depends on the number of lines of the magnetic field cut by the moving surface (PA).

The voltage difference between the two contact surfaces after sliding is shown in Fig. 6, where their values showed relatively higher values than that measured for contact-separation. The highest voltage values were 5100, 4300 and 3500 mV at 0, 120 and 240 mG magnetic field strength respectively. The arrangement of the magnets displayed insignificant effect on voltage values. The same trend shown for contact-separation was observed in sliding condition, where the highest voltage was at 0.2 mm SR thickness. Based on this observation, it seems that voltage values were much influenced by the SR thickness.

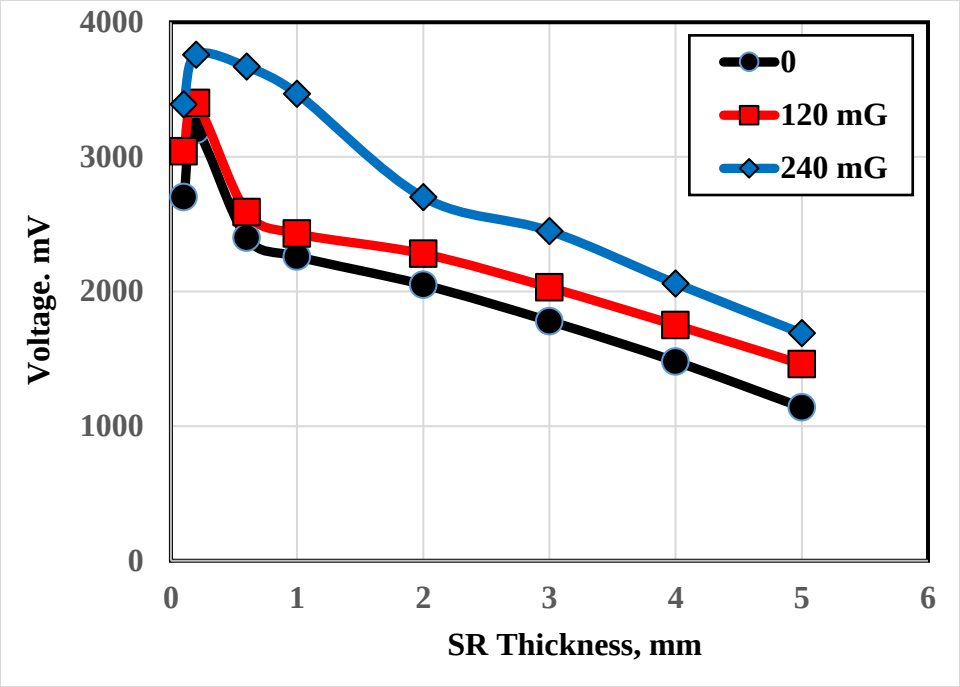

Fig. 5 Voltage difference between PA and SR after contact-separation as function of SR thickness.

It is known that when two dissimilar materials are rubbed together, the two surfaces are electrically charged, where the first becomes positively charged, while the other becomes negatively charged. The intensity of the generated ESC depends on the gap between the surfaces in the triboelectric series. The double layer of ESC on the two sliding surfaces generates electric field. SR as insulator contains ESC that are conserved. ESC would generate an electric field inside the matrix of SR. Presence of the permanent magnet inside SR matrix would help generate extra ESC on the two surfaces. As the permanent magnets are close to the surface the electric field intensity increases.

The influence of the thickness of the SR on the value of ESC can be explained on the bases that sliding of materials as well contact-separation cause the ESC transfer to build up on the two surfaces. In some conditions, ESC may continue to increase, and sometimes it may decrease. ESC variations versus sliding distance propose that ESC does not always build up continuously as sliding proceeds. These variations could be due to random contamination caused by the material transfer of the second surface. Besides, material transfer and surface distortion significantly affect ESC transfer. The surface deformation that occurs during contact-separation and sliding disturbs the electron transfer. It is well known that as the thickness of the SR increased, the deformation increased.

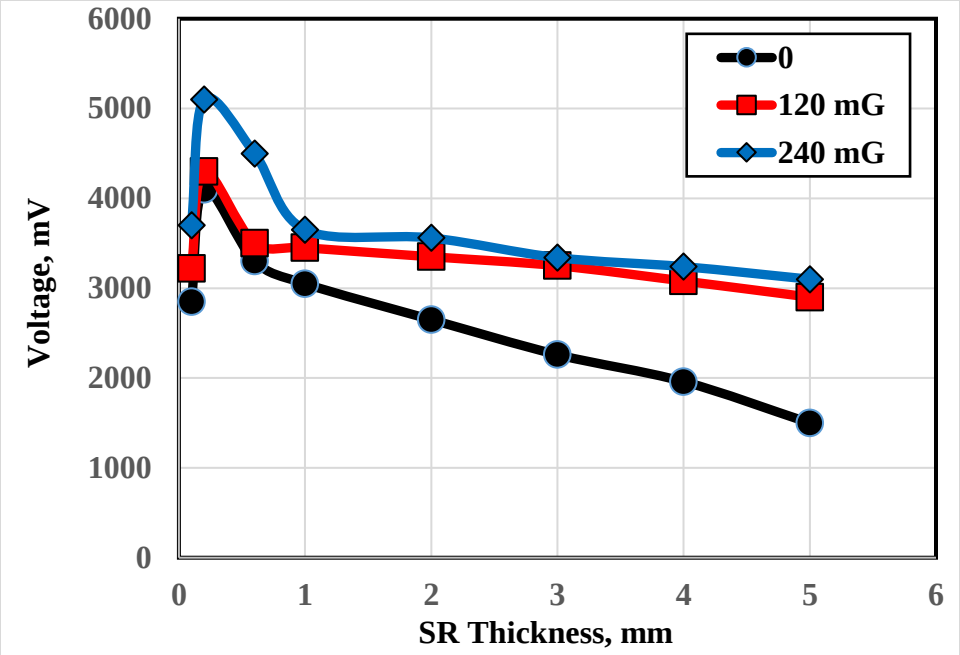

Fig. 6 Voltage difference between PA and SR after sliding as function of SR thickness.

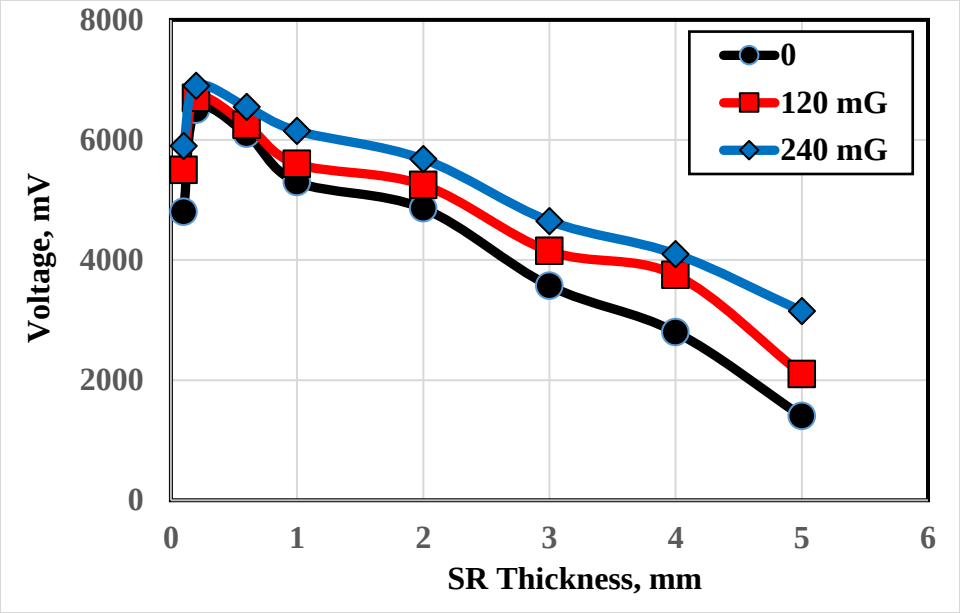

Fig. 7 Voltage difference between Al and SR after contact-separation as function of SR thickness.

Replacing the dielectric surface (PA) by Al film showed the same trend observed for PA after contact-separation and sliding, Figs. 7 and 8 respectively. The maximum voltage values were observed at SR of 0.2 mm thickness. As the magnetic field increased, the voltage increased. In condition of using PMMA instead of Al, voltage values significantly increased after both contact-separation and sliding, Figs. 9 and 10. The increase of the voltage values can be

attributed to the fact that SR is ranked as negative charged material, while PMMA is positive charged one. The gap between SR and PMMA in the triboelectric series is relatively long, therefore, the voltage difference remarkably increases. The long gap between the two sliding surfaces gives higher chance to exchange more electrons between the two contact surfaces. The increase of the mobility of the free electrons to one of the contact surfaces increases ESC. Inserting the magnet under SR matrix would generate extra ESC on the sliding surface.

The fourth TENG investigates the effect of the thickness of Al film of different thickness sliding on PMMA sheet, Fig. 3. At contact-separation, as the thickness of Al increased, voltage decreased, Fig. 11. Besides, the voltage increased with increasing magnetic field intensity. At sliding, the same trend was observed with slight increase in the generated voltage, Fig. 12. The voltage decrease accompanied to the increase of the thickness of contact surfaces may be attributed to the surface straining, where strain can influence charge transfer and can also reverse the direction of charge transfer in some conditions, [37]. It seems the internal strains inside the material may alter the charge transfer direction. Besides, severe rubbing of materials can introduce strains, and consequently affect the charge signal. In addition, strain may alter the type of species transferred during triboelectrification. In contact-separation, it seems that change in the contact area of the two surfaces can alter the magnitude of charging. The material transfer from one surface to the other should not be ignored in explaining the variation of the generated voltage after contact-separation and sliding of the two contact surfaces.

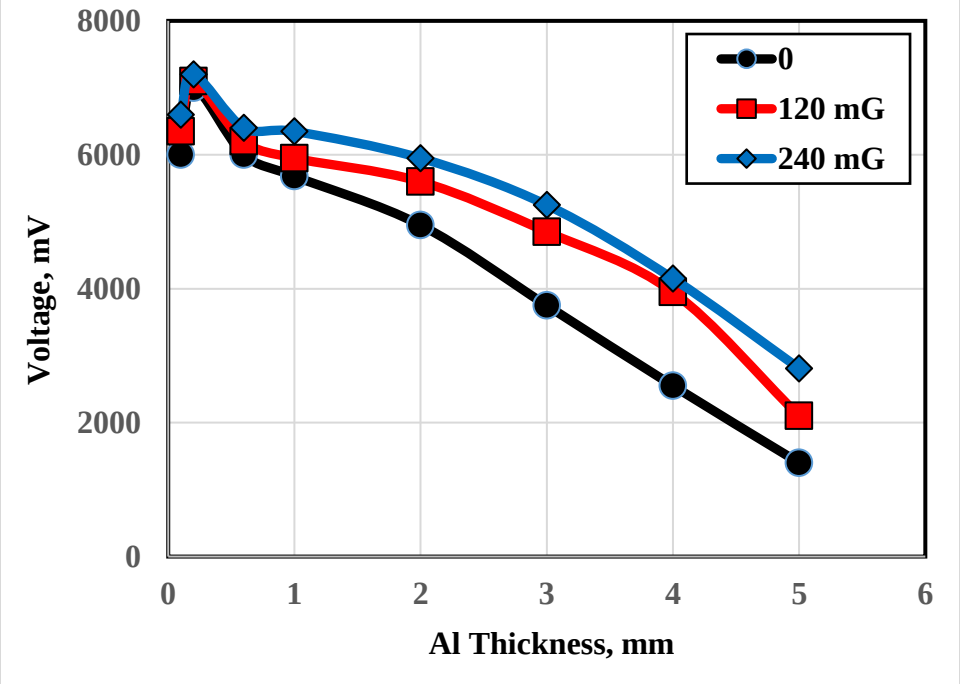

Fig. 8 Voltage difference between Al and SR after sliding as function of SR thickness.

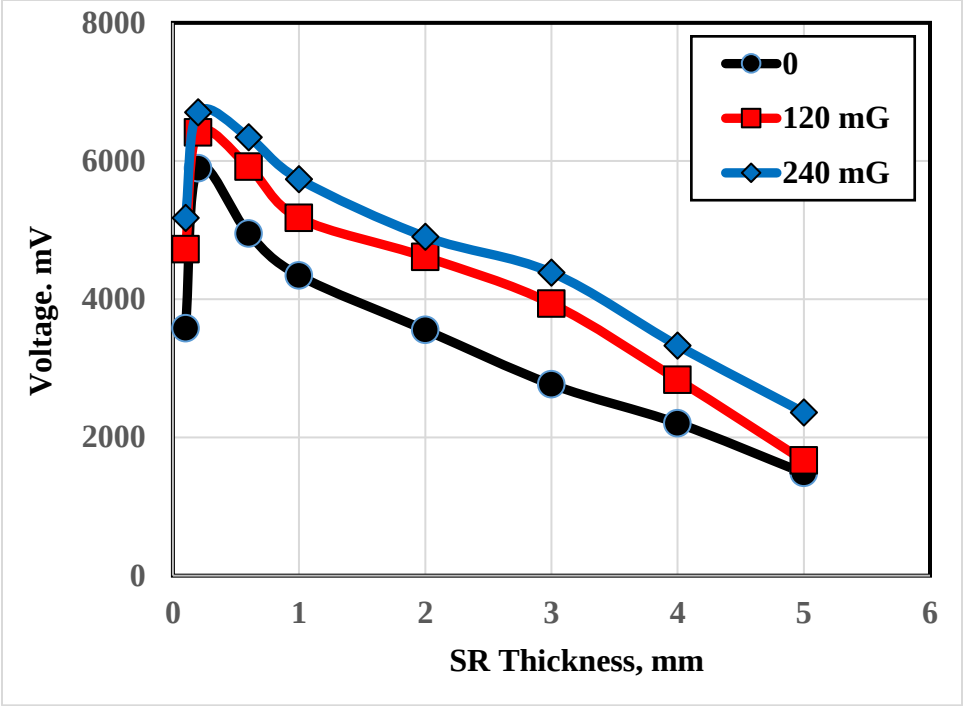

Fig. 9 Voltage difference between PMMA and SR after contact-separation as function of SR thickness.

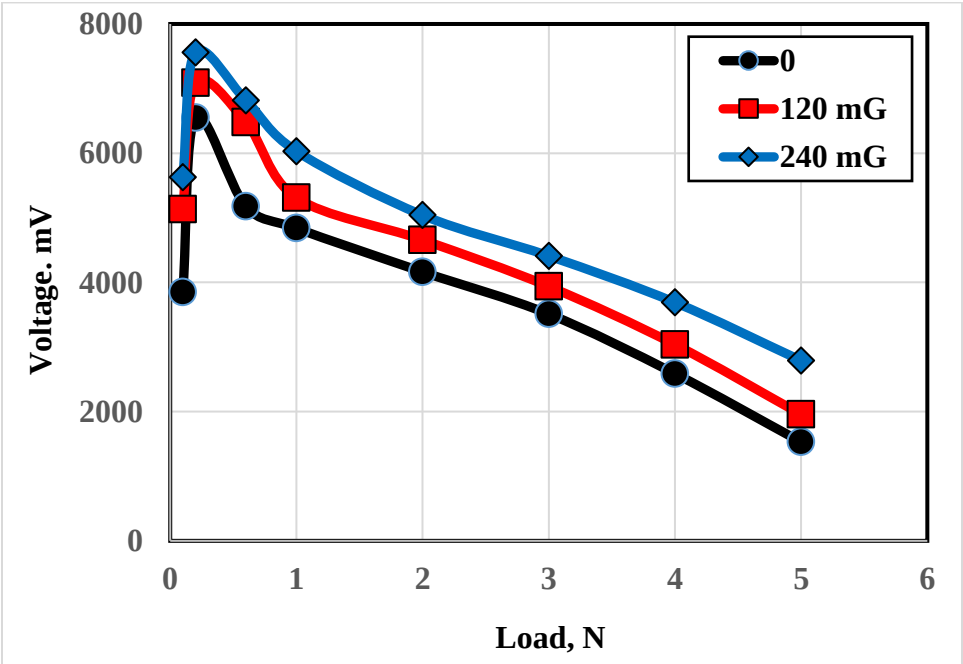

Fig. 10 Voltage difference between PMMA and SR after sliding as function of SR thickness.

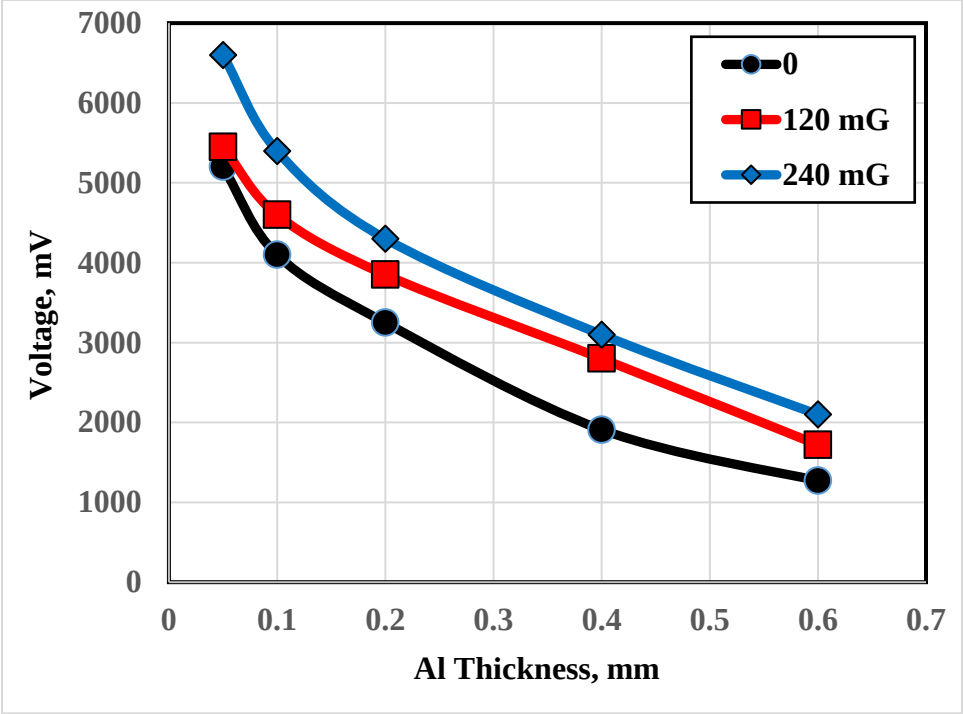

Fig. 11 Voltage difference between Al and PMMA after contact-separation as function of Al thickness.

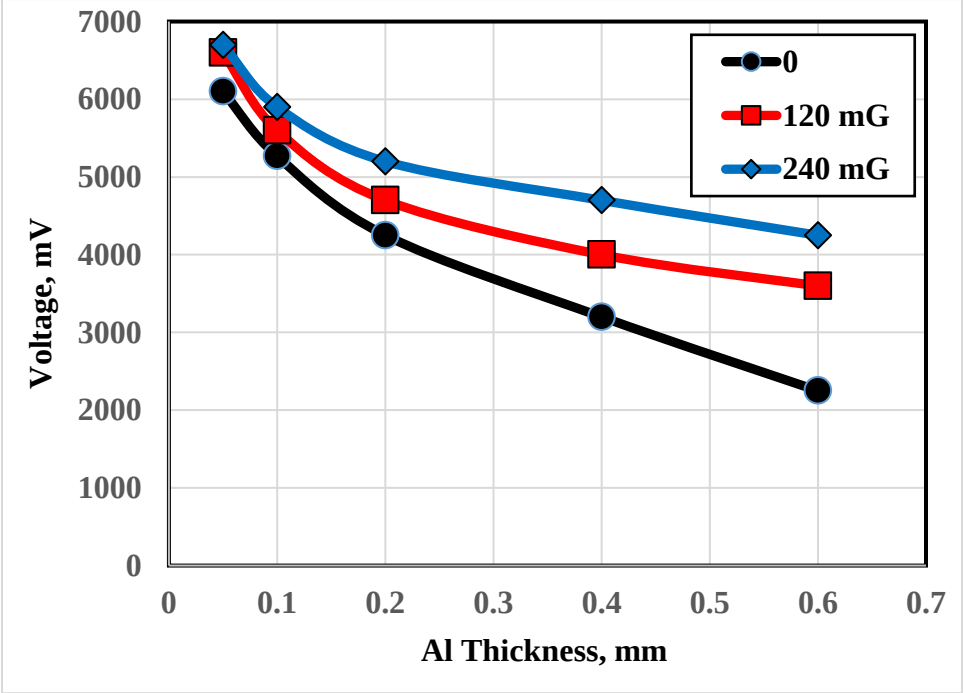

Fig. 12 Voltage difference between Al and PMMA after sliding as function of Al thickness.

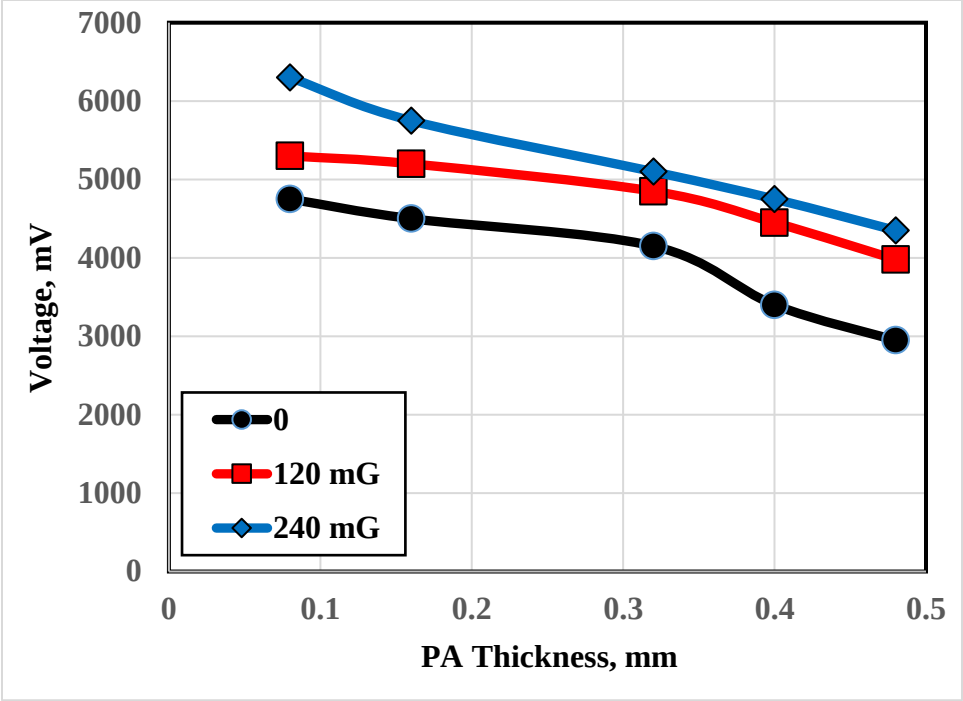

Fig. 13 Voltage difference between PA and PTFE after contact-separation as function of PA thickness.

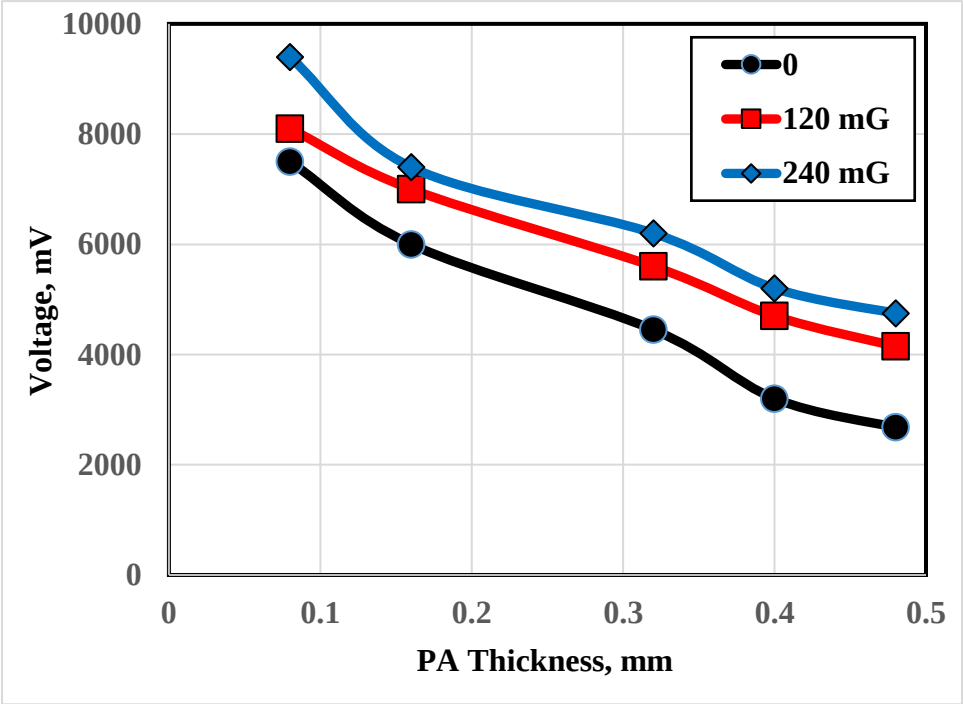

Fig. 14 Voltage difference between PA and PTFE after sliding as function of PA thickness.

In the fifth TENG, Al film was replaced by PA of different thickness sliding on PTFE sheet. The results ESC generated after contact-separation and sliding are shown in Figs. 13 and 14

respectively. The voltage values were relatively higher than displayed by Al film at sliding, Fig. 14, where the highest values were 7500, 8100 and 9400 mV at 0, 120 and 240 mG magnetic strength respectively. The significant voltage increase displayed by PA may be from its rank in the triboelectric series that predict the polarity of the charge transferred from one surface to the other, where the gap between PA and PTFE is quite long. It is obvious that when two dissimilar materials rub each other, the upper material in the triboelectric series gets positively charged and the lower one gets negatively charged.

CONCLUSIONS

1. ESC drastically decreased with increasing silicon rubber thickness. That behavior may be attributed to the material transfer from one surface to the second one.
2. After contact-separation, the changes in the topography of the contact area of the two surfaces can change the magnitude of charging.
3. At sliding, rubbing of the materials causes strains that limits the electron transfer and reverse their direction.
4. As the thickness of the contact surfaces increased, deformation increased and consequently the internal strains, in the matrix of the material that alter the charge transfer direction, increased.
5. ESV increased with increasing the magnetic field.
6. Replacing PA by Al film showed the same trend after contact-separation and sliding, where the generated ESC decreased with increasing their thickness.

REFERENCES

1. El-Shazly M. H., Al-Kabbany A. M., Ali W. Y., Ali A. S. and Ameer A. K., "Influence of Magnetic Field on the Performance of the Triboelectric Nanogenerator", Journal of the Egyptian Society of Tribology, Vol. 21, No. 1, January 2024, pp. 12 – 23, (2024).
2. El-Shazly M. H., Al-Kabbany A. M. and Ali W. Y., Ali A. S. and Massoud M. A., "Effect of the Direction of the Magnetic Field Lines on the Voltage Output of a Triboelectric Nanogenerator", Journal of the Egyptian Society of Tribology, Vol. 20, No. 4, October 2023, pp. 65 – 76, (2023).
3. El-Shazly M. H., Al-Kabbany A. M. and Ali W. Y., Ali A. S. and Massoud M. A., "Effect of the Direction of the Magnetic Field Lines on the Voltage Output of a Triboelectric Nanogenerator", Journal of the Egyptian Society of Tribology, Vol. 20, No. 4, October 2023, pp. 65 – 76, (2023).
4. Elzayady N., Al-Kabbany A. M., Ali W. Y., Ali A. S. and Hamdy K., "Enhancing the Performance of the Triboelectric Nanogenerator", Journal of the Egyptian Society of Tribology, Vol. 20, No. 4, October 2023, pp. 77 – 87, (2023).
5. Ali A. S., Youssef M. M., Ali W. Y. and Elzayady N., "Triboelectric Nanogenerator Based on Contact and Separation as well as Sliding of Polyamide on Polytetrafluoroethelene", Journal of the Egyptian Society of Tribology, Vol. 20, No. 1, January 2023, pp. 32 – 40, (2023).
6. Ali A. S., Youssef M. M., Ali W. Y. and Rashed A., "Enhancing the Efficiency of Triboelectric Nanogenerator by Electrostatic Induction", Journal of the Egyptian Society of Tribology, Vol. 20, No. 1, January 2023, pp. 41 – 50, (2023).
7. El-Shazly M. H., Al-Kabbany A. M., Ali W. Y., Ali A. S. and Massoud M. A., "Effect of Magnetic Field on the Voltage Output of Triboelectric Nanogenerator", Journal of the Egyptian Society of Tribology, Vol. 20, No. 3, July 2023, pp. 85 – 94, (2023).

8. Ali A. S., Youssef M. M., Ali W. Y. and Rashed A., "Triboelectric Nanogenerator Based on Triboelectrification and Magnetic Field", Journal of the Egyptian Society of Tribology, Vol. 20, No. 2, April 2023, pp. 1 – 12, (2023).
9. Gabor D., Radu S. M., Ghicioi E., Paraian M., Jurca A. M., Vatavu N., Paun F., and Popa C. M., "Study of methods for assessment of the ignition risk of dust/air explosive atmospheres by electrostatic discharge", Calitatea, Vol. 20, No. S1, p. 93, (2019).
10. Glor M., and Thurnherr P., "Ignition Hazards Caused by Electrostatic Charges in Industrial Processes", Thuba Ltd, (2015).
11. Von Pidoll U., "An overview of standards concerning unwanted electrostatic discharges", Journal of Electrostatics, Vol. 67, No. 2-3, pp. 445 - 452, (2009).
12. Tian H., and Lee J. J., "Electrostatic discharge damage of MR heads", IEEE transactions on magnetics, Vol. 31, No. 6, pp. 2624 - 2626, (1995).
13. Al-Kabbany A. M., and Ali W. Y., "Reducing the Electrostatic Charge of Polyester by Blending by Polyamide Strings", Journal of the Egyptian Society of Tribology, Vol. 16, No. 4, pp. 36 - 44, (2019).
14. Ali A. S., Al-Kabbany A. M., Ali W. Y., and Samy A. M., "Reducing the Electrostatic Charge Generated from Sliding of Rubber on Polyethylene Artificial Turf", Journal of the Egyptian Society of Tribology, Vol. 17, No. 2, pp. 40 - 49, (2020).
15. Ali A. S., El-Sherbiny Y. M., Ali W. Y., and Ibrahem R. A., "Selection of Floor Materials in Hospitals to Resist Covid-19", Journal of the Egyptian Society of Tribology, Vol. 18, No. 1, pp. 40 - 51, (2021).
16. Ali A. S., Al-Kabbany A. M., Ali W. Y., and Badran A. H., "Triboelectrified Materials of Facemask to Resist Covid-19", Journal of the Egyptian Society of Tribology, Vol. 18, No. 1, pp. 52 - 62, (2021).
17. Ali A. S., Al-Kabbany A. M., Ali W. Y., and Ibrahem R. A., "Proper Material Selection of Medical Safety Goggles", Journal of the Egyptian Society of Tribology, Vol. 18, No. 2, pp. 1 - 14, (2021).
18. Al-Kabbany A. M., Ali W. Y., and Ali A. S., "Proposed Materials for Face Masks", Journal of the Egyptian Society of Tribology, Vol. 18, No. 3, pp. 35 - 41, (2021).
19. Al-Kabbany A. M., Ali W. Y., and Ali A. S., "Proper Selection Materials of Face Shields, Eyeglasses and Goggles", Journal of the Egyptian Society of Tribology, Vol. 18, No. 3, pp. 42 - 51, (2021).
20. Furfari F. A., "A history of the Van de Graaff generator", IEEE Industry Applications Magazine, Vol. 11, No. 1, pp. 10–14, (2005).
21. Fan F.-R., Tian Z.-Q., and Wang Z. L., "Flexible triboelectric generator", Nano Energy, Vol. 1, No. 2, pp. 328 - 334, (2012).
22. Goh Q. L., Chee P., Lim E. H., and Liew G. G., "Self-powered pressure sensor based on microfluidic triboelectric principle for human–machine interface applications", Smart Materials and Structures, Vol. 30, No. 7, p. 075012, (2021).
23. Zhang R., Hummelgard M., Ortegren J., Olsen M., Andersson H., Yang ¨ Y., Olin H., and Wang Z. L., "Utilising the triboelectricity of the human body for human-computer interactions", Nano Energy, Vol. 100, , p. 107503, (2022).
24. Yang Y., Zhu G., Zhang H., Chen J., Zhong X., Lin Z.-H., Su Y., Bai P., Wen X., and Wang Z. L., "Triboelectric nanogenerator for harvesting wind energy and as self-powered wind vector sensor system", ACS nano, Vol. 7, No. 10, pp. 9461 - 9468, (2013).

25. Han J., Feng Y., Chen P., Liang X., Pang H., Jiang T., and Wang Z. L., "Wind-driven soft-contact rotary triboelectric nanogenerator based on rabbit fur with high performance and durability for smart farming", Advanced Functional Materials, Vol. 32, No. 2, p. 2108580, (2022).
26. Zhang H., Yang Y., Su Y., Chen J., Adams K., Lee S., Hu C., and Wang Z. L., "Triboelectric nanogenerator for harvesting vibration energy in full space and as self-powered acceleration sensor", Advanced Functional Materials, Vol. 24, No. 10, pp. 1401 - 1407, (2014).
27. Cheng P., Guo H., Wen Z., Zhang C., Yin X., Li X., Liu D., Song W., Sun X., Wang J., et al., "Largely enhanced triboelectric nanogenerator for efficient harvesting of water wave energy by soft contacted structure", Nano Energy, Vol. 57, pp. 432 - 439, (2019).
28. Meng B., Tang W., Too Z.-h., Zhang X., Han M., Liu W., and Zhang H., "A transparent single-friction-surface triboelectric generator and selfpowered touch sensor", Energy & Environmental Science, Vol. 6, No. 11, pp. 3235 - 3240, (2013).
29. Lei H., Xiao J., Chen Y., Jiang J., Xu R., Wen Z., Dong B., and Sun X., "Bamboo-inspired self-powered triboelectric sensor for touch sensing and sitting posture monitoring", Nano Energy, Vol. 91, p. 106670, (2022).
30. Pu X., Tang Q., Chen W., Huang Z., Liu G., Zeng Q., Chen J., Guo H., Xin L., and Hu C., "Flexible triboelectric 3D touch pad with unit subdivision structure for effective XY positioning and pressure sensing", Nano Energy, Vol. 76, p. 105047, (2020).
31. Haque R. I., Chandran O., Lani S., and Briand D., "Self-powered triboelectric touch sensor made of 3D printed materials", Nano Energy, Vol. 52, pp. 54 - 62, (2018).
32. Chen Y., Cheng Y., Jie Y., Cao X., Wang N., and Wang Z. L., "Energy harvesting and wireless power transmission by a hybridized electromagnetic–triboelectric nanogenerator", Energy & Environmental Science, Vol. 12, No. 9, pp. 2678 - 2684, (2019).
33. Quan T., Wang Z. L., and Yang Y., "A shared-electrode-based hybridized electromagnetic-triboelectric nanogenerator", ACS Applied Materials & Interfaces, Vol. 8, No. 30, pp. 19 573 - 19 578, (2016).
34. Qin K., Chen C., Pu X., Tang Q., He W., Liu Y., Zeng Q., Liu G., Guo H., and Hu C., "Magnetic array assisted triboelectric nanogenerator sensor for real-time gesture interaction", Nano-micro letters, Vol. 13, pp. 1 - 9, (2021).
35. Ali A. S., Al-Kabbany A. M., and Ali W. Y., "Voltage Generated From Triboelectrification of Rabbit Fur and Polymeric Materials", Journal of the Egyptian Society of Tribology, Vol. 19, No. 3, pp. 10 - 18, (2022).
36. Zhang R., and Olin H., "Material choices for triboelectric nanogenerators: a critical review", EcoMat, Vol. 2, No. 4, p. e12062, (2020).
37. Sow, M., Lacks, D. J., Sankaran, R. M., "Effects of material strain on triboelectric charging: Influence of material properties", Journal of Electrostatics 71 pp. 396 – 399, (2013).